

Dynamic modeling and analysis of brucellosis on metapopulation network: Heilongjiang as cases

Xin Pei(裴鑫), Xuan-Li Wu(武绚丽), Pei Pei(裴沛), Ming-Tao Li(李明涛), Juan Zhang(张娟), and Xiu-Xiu Zhan(詹秀秀)

Citation: Chin. Phys. B, 2025, 34 (**1**): 018904. DOI: 10.1088/1674-1056/ad92ff

What follows is a list of articles you may be interested in

Detecting the core of a network by the centralities of the nodes

Peijie Ma(马佩杰), Xuezao Ren(任学藻), Junfang Zhu(朱军芳), and Yanqun Jiang(蒋艳群)

Chin. Phys. B, 2024, 33 (**8**): 088903. DOI: 10.1088/1674-1056/ad4cd4

A multilayer network diffusion-based model for reviewer recommendation

Yiwei Huang(黄羿炜), Shuqi Xu(徐舒琪), Shimin Cai(蔡世民), and Linyuan Lü(吕琳媛)

Chin. Phys. B, 2024, 33 (**3**): 038901. DOI: 10.1088/1674-1056/ad181d

Analysis of radiation diffusion of COVID-19 driven by social attributes

Fuzhong Nian(年福忠), Xiaochen Yang(杨晓晨), and Yayong Shi(师亚勇)

Chin. Phys. B, 2024, 33 (**1**): 018904. DOI: 10.1088/1674-1056/acd7d1

Self-similarity of complex networks under centrality-based node removal strategy

Dan Chen(陈单), Defu Cai(蔡德福), and Housheng Su(苏厚胜)

Chin. Phys. B, 2023, 32 (**9**): 098903. DOI: 10.1088/1674-1056/acd3e2

Identification of key recovering node for spatial networks

Zijian Yan(严子健), Yongxiang Xia(夏永祥), Lijun Guo(郭丽君), Lingzhe Zhu(祝令哲), Yuanyuan Liang(梁圆圆), and Haicheng Tu(涂海程)

Chin. Phys. B, 2023, 32 (**6**): 068901. DOI: 10.1088/1674-1056/acb75f

---

SPECIAL TOPIC — Computational programs in complex systems

Dynamic modeling and analysis of brucellosis on metapopulation network: Heilongjiang as cases

Xin Pei(裴鑫)[1], Xuan-Li Wu(武绚丽)[1], Pei Pei(裴沛)[2], Ming-Tao Li(李明涛)[1], Juan Zhang(张娟)[3], and Xiu-Xiu Zhan(詹秀秀)[4,†]

[1] *School of Mathematics, Taiyuan University of Technology, Taiyuan* 030024, *China*
[2] *Department of Information Technology, Shanxi Professional College of Finance, Taiyuan* 030008, *China*
[3] *Complex System Research Center, ShanXi University, Taiyuan* 030006, *China*
[4] *Alibaba Complex Science Research Center, Hangzhou Normal University, Hangzhou* 311121, *China*

(Received 29 September 2024; revised manuscript received 4 November 2024; accepted manuscript online 15 November 2024)

Livestock transportation is a key factor that contributes to the spatial spread of brucellosis. To analyze the impact of sheep transportation on brucellosis transmission, we develop a human–sheep coupled brucellosis model within a metapopulation network framework. Theoretically, we examine the positively invariant set, the basic reproduction number, the existence, uniqueness, and stability of disease-free equilibrium and the existence of the endemic equilibrium of the model. For practical application, using Heilongjiang province as a case study, we simulate brucellosis transmission across 12 cities based on data using three network types: the BA network, the ER network, and homogeneous mixing network. The simulation results indicate that the network's average degree plays a role in the spread of brucellosis. For BA and ER networks, the basic reproduction number and cumulative incidence of brucellosis stabilize when the network's average degree reaches 4 or 5. In contrast, sheep transport in a homogeneous mixing network accelerates the cross-regional spread of brucellosis, whereas transportation in a BA network helps to control it effectively. Furthermore, the findings suggest that the movement of sheep is not always detrimental to controlling the spread of brucellosis. For cities with smaller sheep populations, such as Shuangyashan and Qitaihe, increasing the transport of sheep outward amplifies the spatial spread of the disease. In contrast, in cities with larger sheep populations, such as Qiqihar, Daqing, and Suihua, moderate sheep outflow can help reduce the spread. In addition, cities with large livestock populations play a dominant role in the overall transmission dynamics, underscoring the need for stricter supervision in these areas.

Keywords: brucellosis, metapopulation network, basic reproduction number, sheep transport

PACS: 89.75.Hc, 05.90.+m, 92.20.jp, 02.70.–c

DOI: 10.1088/1674-1056/ad92ff **CSTR:** 32038.14.CPB.ad92ff

1. Introduction

Brucellosis is a zoonotic infectious disease that can manifest in acute and chronic forms. Cattle and sheep serve as the primary hosts for brucella bacteria in livestock, while humans and other susceptible individuals are usually infected by direct contact with infected animals or exposure to brucella bacteria in contaminated environments.[1] Examining the data on the incidence of human brucellosis in China over the past 20 years (see Fig. 1), a noticeable decline in the number of cases began around 2015–2016. The data in Fig. 1 comes from the Chinese Center for Disease Control and Prevention Information System, with the link https://www.chinacdc.cn/. This trend suggests that efforts to prevent and control brucellosis have achieved initial success. However, the number of cases rebounded in 2019 and has since remained at a high level. Spatially, brucellosis has spread to all provinces in China, showing a trend from east to west, south to north, and from traditional pastoral and semi-pastoral areas to non-pastoral areas. Based on their prevalence, they are divided into severely epidemic areas, generally epidemic areas, and sporadic epidemic areas. The cross-regional transportation of animals has led to the spread of brucella in urban and other spatial areas, thus increasing the number of cases of brucellosis and its spatial spread.[2,3] In recent years, although China has introduced

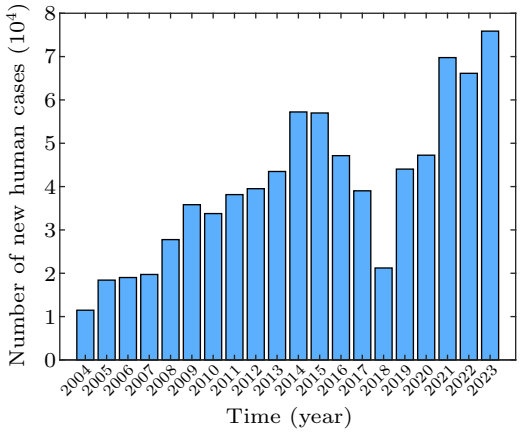


Fig. 1. Number of human brucellosis cases in China from 2004 to 2023.

†Corresponding author. E-mail: zhanxiuxiu@hznu.edu.cn

© 2025 Chinese Physical Society and IOP Publishing Ltd. All rights, including for text and data mining, AI training, and similar technologies, are reserved.

many measures to control brucellosis, the continuous increase in animal breeding and frequent animal transport have resulted in an upward trend in brucellosis cases, which has severely impacted the health of the Chinese people and caused significant disruptions to the livestock industry.[4,5] For example, Ge, Suo and Yin *et al.* have studied the situation of brucellosis in Heilongjiang province, finding that the incidence of human brucellosis in Heilongjiang has shown a downward trend in recent years, but further strengthening of prevention and control efforts is still necessary.[6–8] Therefore, considering the transportation of animals between regions, studying the interregional transmission of brucellosis becomes an urgent task.

Patch dynamics models are essential tools for studying the spatial transmission of brucellosis, and significant progress has been made in this field. These models have contributed to a deeper understanding of how the disease spreads across different spatial regions. For example, Zhang *et al.*[4] proposed a n-patch dynamic model to investigate the impact of the dispersal of cows in Zhejiang province on the transmission of brucellosis in 2014. They found that the dispersal of susceptible populations and the centralization of infected cattle to areas with a large breeding scale were beneficial for the control of the epidemic. In 2017, Yang *et al.*[9] established a nonlinear modeling framework based on spatial simulation of patch structure to study the spread of brucellosis, emphasizing the importance of spatial heterogeneity in brucellosis prevention and control. In 2022, Guo *et al.*[10] explored the impact of sheep transportation on brucellosis transmission using a multi-patch model, with a case study focusing on the spread of the disease between Ulanhot City and Jalad Banner. Their findings indicated that regulation of sheep transport was an effective measure for preventing and controlling brucellosis. Qin *et al.*[11] developed a human–sheep coupled brucellosis model based on patch dynamics and examined the impact of sheep movement on the transmission of brucellosis. Their study was based on human brucellosis data from Shanxi and Hebei provinces between 2010 and 2018. From the perspective of the transmission process and contact patterns of diseases, the above models are all homogeneous mixing dynamics models, which means that livestock transport between regions is equally possible. However, livestock transport exhibits spatial heterogeneity due to differences in breeding volumes and socio-economic conditions in reality. To more effectively control the spread, complex network theory provides new perspectives and approaches for studying the mechanisms of epidemic transmission.[12–14] The metapopulation model, an essential tool in this context, divides a single population into n spatially discrete subpopulations or patches based on geographical areas. Within each subpopulation, individuals are homogeneously mixed, while the subpopulations themselves are connected heterogeneously.[15–17] This model is particularly advantageous as it allows for the study of how individual movements influence the transmission of diseases across spatially separated populations.

Given the significant impact of livestock transportation on the spatial spread of brucellosis and the current state of research, we construct a human–sheep coupling brucellosis model in the metapopulation network[18,19] to study the effect of goat transportation on brucellosis transmission. The structure of the paper is as follows. In Section 2, we construct a human–sheep coupling brucellosis model on a metapopulation network for sheep transportation between nodes (cities). In Section 3, we perform a theoretical analysis of the model, including the basic reproduction number, the positively invariant set, the existence and global asymptotic stability of the disease-free equilibrium point, and the existence of the endemic equilibrium point. In Section 4, taking the 12 regions in Heilongjiang province as examples, numerical simulations are carried out. In Section 5, a brief conclusion is made.

2. Model formulation

To study the impact of livestock transportation on the spread of brucellosis, we propose a human–sheep coupling brucellosis model on a metapopulation network. In the model, sheep are divided into three classes, that is, susceptible sheep (S), exposed sheep (E), and infected sheep (I), the human population can be divided into two categories, that is, susceptible humans (S_h) and infected humans (I_h). In addition, the sheep and humans within each subpopulation are homogeneously mixed, and the edges between subpopulations represent the transportation of sheep between them, with these edges being heterogeneous as shown in Fig. 2. We show the state change of the model in Fig. 3, and the details of the model are shown below.

(i) Brucella-infected sheep, including both exposed and infected sheep, release the bacteria into the environment during illness. Since infected sheep show clinical symptoms and are culled, they are not considered for animal transport.

(ii) Susceptible sheep can become infected by contact with exposed or infected sheep during the latent period or by encountering brucella in the environment. Assuming equal pathogenicity between exposed and infected sheep, the infection rate remains consistent for both susceptible humans and sheep when they come into contact with them.

(iii) Humans can only be infected through contact with brucella in the environment, exposed sheep, or infected sheep. Infected humans do not transmit the disease but may experience natural death. Due to the low mortality rate associated with brucellosis, disease-related mortality is not considered in this context.

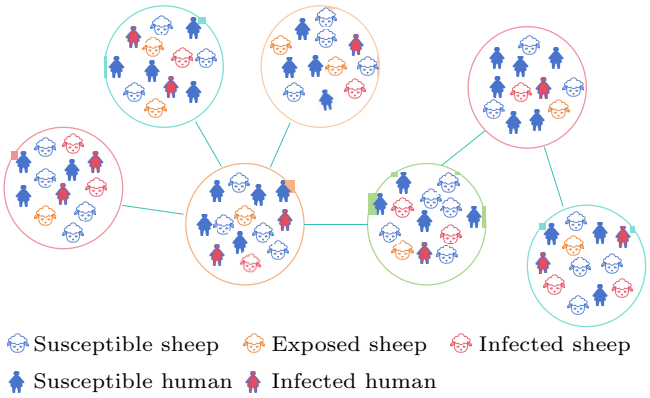


Fig. 2. Schematic diagram of the metapopulation network. Each subpopulation contains homogeneous mix of sheep and humans, and the edges between subpopulations represent the transportation of sheep between them.

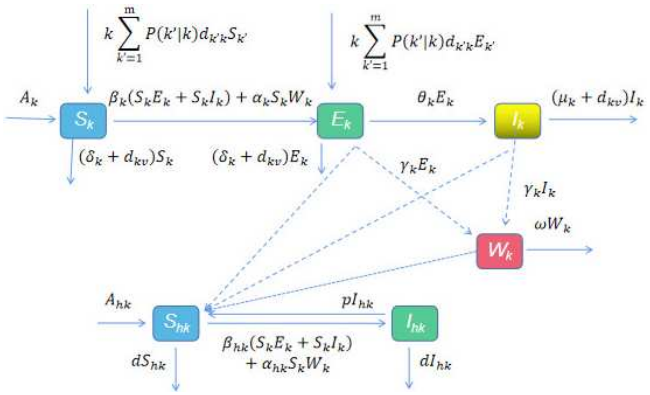


Fig. 3. Flow chart of the brucellosis coupled metapopulation model of humans and sheep.

According to Fig. 3, the model can be described as follows:

$$\begin{cases}
\frac{dS_k}{dt} = A_k - \beta_k(S_kE_k + S_kI_k) - \alpha_k S_k W_k - d_{kv}S_k - \delta_k S_k \\
\qquad + k\sum_{k'=1}^{m} P(k|k')d_{k'k}S_{k'}, \\
\frac{dE_k}{dt} = \beta_k(S_kE_k + S_kI_k) + \alpha_k S_k W_k - \delta_k E_k - \theta_k E_k \\
\qquad - d_{kv}E_k + k\sum_{k'=1}^{m} P(k|k')d_{k'k}E_{k'}, \\
\frac{dI_k}{dt} = \theta_k E_k - \mu_k I_k - d_{kv}I_k, \\
\frac{dW_k}{dt} = \gamma_k(E_k + I_k) - \omega W_k, \\
\frac{dS_{hk}}{dt} = A_{hk} - \beta_{hk}(E_kS_{hk} + I_kS_{hk}) - \alpha_{hk}W_kS_{hk} - dS_{hk} + pI_{hk}, \\
\frac{dI_{hk}}{dt} = \beta_{hk}(E_kS_{hk} + I_kS_{hk}) + \alpha_{hk}W_kS_{hk} - dI_{hk} - pI_{hk},
\end{cases} \tag{1}$$

where m represents the maximum value of node degree. S_k, E_k, I_k, and W_k denote the average numbers of susceptible sheep, latent sheep, infected sheep, and brucella bacteria in subpopulations of degree k. S_{hk} and I_{hk} represent the average numbers of susceptible humans and infected humans in subpopulations of degree k. A_k and A_{hk} indicate the average births of susceptible sheep and susceptible individuals in subpopulations of degree k. $P(k'|k)$ denotes the conditional probability that a node with degree k connects to a node with degree k'. $d_{k'k}$ represents the migration rate of sheep from a subpopulation of degree k' to a subpopulation of degree k in a unit of time. The meaning of parameters involved in system (1) is shown in Tables 1 and 2.

3. Dynamic analysis of model

Since the first four equations of system (1) are independent of the last two equations, we only study the following system for the dynamic analysis of system (1):

$$\begin{cases}
\frac{dS_k}{dt} = A_k - \beta_k(S_kE_k + S_kI_k) - \alpha_k S_k W_k - d_{kv}S_k \\
\qquad - \delta_k S_k + k\sum_{k'=1}^{m} P(k|k')d_{k'k}S_{k'}, \\
\frac{dE_k}{dt} = \beta_k(S_kE_k + S_kI_k) + \alpha_k S_k W_k - \delta_k E_k - \theta_k E_k \\
\qquad - d_{kv}E_k + k\sum_{k'=1}^{m} P(k|k')d_{k'k}E_{k'}, \\
\frac{dI_k}{dt} = \theta_k E_k - \mu_k I_k - d_{kv}I_k, \\
\frac{dW_k}{dt} = \gamma_k(E_k + I_k) - \omega W_k.
\end{cases} \tag{2}$$

Theorem 1 Let $d_v = \min\{d_{kv}, 1 \le k \le m\}$, $\gamma = \max\{\gamma_k, 1 \le k \le m\}$, $N^* = A/d_v$, where $A = \sum_{k'=1}^{m} A_{k'}$. Every set of solution G of system (2) satisfies $\{(S,E,I,W) \in R_+^{4m} : \sum_{k'=1}^{m}(S_k + E_k + I_k) \le N^*, \sum_{k'=1}^{m} W_k \le \gamma N^*/\omega\}$, which is a positive invariant set of system (2).

Proof Firstly, summing the first three equations of system (2) over nodes of degree k yields

$$\begin{aligned}
N_k' &= (S_k + E_k + I_k)' \\
&= A_k - d_{kv}N_k - \mu_k I_k - \delta_k(S_k + E_k) \\
&\quad + k\sum_{k'=1}^{m} P(k|k')d_{k'k}(S_{k'} + E_{k'}).
\end{aligned}$$

According to the migration relationships between the nodes, the following relationships can be derived:

$$\delta_k = \sum_{k'=1}^{m} k'P(k'|k)d_{kk'}, \quad 1 \le k \le m. \tag{3}$$

Combining Eq. (3), and summing the first three equations of V nodes yields

$$\begin{aligned}
N' = \sum_{k'=1}^{m} N_k' &= \sum_{k'=1}^{m} (S_k + E_k + I_k)' \\
&= \sum_{k'=1}^{m} (A_{k'} - d_{k'v}N_{k'} - \mu_{k'}I_{k'}) \\
&\le A - d_v N.
\end{aligned}$$

Therefore, $\limsup_{t\to\infty} N \le A/d_v$. Additionally,

$$\begin{aligned}
\sum_{k'=1}^{m} W_{k'}' &= \sum_{k'=1}^{m} (\gamma_{k'}E_{k'} + \gamma_{k'}I_{k'} - \omega W_{k'}) \\
&\le \gamma\sum_{k'=1}^{m} (E_{k'} + I_{k'}) - \omega\sum_{k'=1}^{m} W_{k'} \\
&\le \gamma\frac{A}{d_v} - \omega\sum_{k'=1}^{m} W_{k'}.
\end{aligned}$$

Thus, $\limsup_{t\to\infty}\sum_{k'=1}^{m} W_{k'} \le \frac{\gamma A}{d_v\omega}$.

In conclusion, G is a positively invariant set of system (2).

Theorem 2 The system (2) has a unique disease-free equilibrium point.

Proof Let the right-hand side of system (2) be zero and choose $E_k^0 = I_k^0 = W_k^0 = 0$, we obtain the following system:

$$A_k - d_{kv}S_k^0 - \delta_k S_k^0 + k\sum_{k'=1}^{m} P(k|k')d_{k'k}S_{k'}^0 = 0,\quad 1 \le k \le m. \tag{4}$$

The above equation can also be expressed in the following form:

$$\begin{pmatrix} -d_{1v}-\delta_1 & P(1|2)d_{21} & \dots & P(1|m)d_{m1} \\ 2P(2|1)d_{12} & -d_{2v}-\delta_2 & \dots & 2P(2|m)d_{m2} \\ \vdots & \vdots & \ddots & \vdots \\ mP(m|1)d_{1m} & k_mP(m|2)d_{2m} & \dots & -d_{mv}-\delta_m \end{pmatrix}_{(m\times m)} \times \begin{pmatrix} S_1^0 \\ S_2^0 \\ \vdots \\ S_m^0 \end{pmatrix} = \begin{pmatrix} -A_1 \\ -A_2 \\ \vdots \\ -A_m \end{pmatrix}.$$

Observing the coefficient matrix and combining with Eq. (3), the coefficient matrix of system (4) is strictly diagonally dominant. According to Appendix A in Ref. [20], the negative of the coefficient matrix of system (4) is an irreducible Metzler matrix. By the Perron–Frobenius Theorem, system (4) has a unique non-trivial positive solution. Hence, the disease-free equilibrium point of system (2) exists and is unique, which can be denoted as

$$P_0 = (S_1^0,\dots,S_m^0,0,\dots,0,0,\dots,0).$$

3.1. The basic reproduction number

We calculate the basic reproduction number of system (2) in this section. Based on the definitions of the basic reproduction number and the next-generation matrix in Refs. [20,21], only a set of vectors representing infectious compartments must be considered, denoted $x = (E_1,\dots,E_m,I_1,\dots,I_m,W_1,\dots,W_m)^{\mathrm{T}}$. Therefore, we consider the following auxiliary system:

$$\begin{cases} \frac{\mathrm{d}E_k}{\mathrm{d}t} = \beta_k(S_kE_k + S_kI_k) + \alpha_kS_kW_k \\ \qquad\quad -\delta_kE_k - \theta_kE_k - d_{kv}E_k + k\sum_{k'=1}^{m} P(k|k')d_{k'k}E_{k'}, \\ \frac{\mathrm{d}I_k}{\mathrm{d}t} = \theta_kE_k - \mu_kI_k - d_{kv}I_k, \\ \frac{\mathrm{d}W_k}{\mathrm{d}t} = \gamma_k(E_k + I_k) - \omega W_k. \end{cases} \tag{5}$$

By the method outlined in Ref. [20], we define

$$\mathcal{F} = \begin{pmatrix} \beta_1(S_1E_1 + S_1I_1) + \alpha_1S_1W_1 \\ \vdots \\ \beta_m(S_mE_m + S_mI_m) + \alpha_mS_mW_m \\ 0 \\ \vdots \\ 0 \\ 0 \\ \vdots \\ 0 \end{pmatrix},$$

$$\mathcal{V} = \begin{pmatrix} \theta_1E_1 + d_{1v}E_1 + \delta_{1v}E_1 - \sum_{k'=1}^{m} P(1|k')d_{k'1}E_{k'} \\ \vdots \\ \theta_mE_m + d_{mv}E_m + \delta_{mv}E_m - m\sum_{k'=1}^{m} P(m|k')d_{k'm}E_{k'} \\ \mu_1I_1 + d_{1v}I_1 - \theta_1E_1 \\ \vdots \\ \mu_mI_m + d_{mv}I_m - \theta_mE_m \\ \omega W_1 - \gamma_1(E_1 + I_1) \\ \vdots \\ \omega W_m - \gamma_m(E_m + I_m) \end{pmatrix}.$$

The partial derivatives of the above column vector with respect to E_k, I_k and W_k at the disease-free equilibrium yield

$$F = \begin{pmatrix} F_1 & F_2 & F_3 \\ 0 & 0 & 0 \\ 0 & 0 & 0 \end{pmatrix}_{(3m\times 3m)},\quad V = \begin{pmatrix} V_1 & 0 & 0 \\ V_2 & V_3 & 0 \\ V_4 & V_5 & V_6 \end{pmatrix}_{(3m\times 3m)},$$

where

$$\begin{aligned} &F_1 = F_2 = \mathrm{diag}(\beta_kS_k^0)_{(m\times m)},\ F_3 = \mathrm{diag}(\alpha_kS_k^0)_{(m\times m)}, \\ &V_1 = \mathrm{diag}(\theta_k + d_{kv})_{(m\times m)} - B, \\ &V_2 = -\mathrm{diag}(\theta_k)_{(m\times m)},\ V_3 = \mathrm{diag}(\mu_k + d_{kv})_{(m\times m)}, \\ &V_4 = V_5 = -\mathrm{diag}(\gamma_k)_{(m\times m)},\ V_6 = \mathrm{diag}(\omega)_{(m\times m)}, \\ &B = \begin{pmatrix} -\delta_{1v} & P(1|2)d_{21} & \cdots & P(1|m)d_{m1} \\ 2P(2|1)d_{12} & -\delta_{2v} & \cdots & 2P(2|m)d_{m2} \\ \vdots & \vdots & \ddots & \vdots \\ mP(m|1)d_{1m} & mP(m|2)d_{2m} & \cdots & -\delta_{mv} \end{pmatrix}. \end{aligned}$$

After computation, we obtain

$$V^{-1} = \begin{pmatrix} V_1^{-1} & 0 & 0 \\ -V_3^{-1}V_2V_1^{-1} & V_3^{-1} & 0 \\ V_6^{-1}(V_5V_3^{-1}V_2V_1^{-1} - V_4V_1^{-1}) & -V_6^{-1}V_5V_3^{-1} & V_6^{-1} \end{pmatrix}_{(3m\times 3m)}. \tag{6}$$

Then,

$$FV^{-1} = \begin{pmatrix} \Delta & F_2V_3^{-1} - F_3V_6^{-1}V_5V_3^{-1} & F_3V_6^{-1} \\ 0 & 0 & 0 \\ 0 & 0 & 0 \end{pmatrix}_{(3m\times 3m)}, \tag{7}$$

where $\Delta = F_1V_1^{-1} - F_2V_3^{-1}V_2V_1^{-1} + F_3V_6^{-1}(V_5V_3^{-1}V_2V_1^{-1} - V_4V_1^{-1})$. So, the basic reproduction number of system (2) is

$$R_0 = \rho(FV^{-1}) = \rho(F_1V_1^{-1} - F_2V_3^{-1}V_2V_1^{-1} + F_3V_6^{-1}(V_5V_3^{-1}V_2V_1^{-1} - V_4V_1^{-1})), \quad (8)$$

where $\rho(FV^{-1})$ represents the spectral radius of the matrix FV^{-1}.

In particular, without considering migration between populations, the basic reproduction number of the subpopulation with degree k is

$$R_{k0} = \frac{S_k^0(\theta_k + \mu_k + d_{kv})(\beta_k\omega + \alpha_k\gamma_k)}{\omega(\theta_k + d_{kv})(\mu_k + d_{kv})}. \quad (9)$$

3.2. The global stability of the disease-free equilibrium

Theorem 3 When $R_0 < 1$, the disease-free equilibrium P^0 of system (2) is globally asymptotically stable in G.

Proof First, we will prove that P^0 is locally asymptotically stable. Define

$$M = F - V = \begin{pmatrix} F_1 - V_1 & F_2 & F_3 \\ -V_2 & -V_3 & 0 \\ -V_4 & -V_5 & -V_6 \end{pmatrix}_{(3m\times 3m)}, \quad (10)$$

and let $s(M)$ be the maximum real part of the eigenvalues of M. According to Theorem 2 in Ref. [20], we have

$$R_0 < 1 \Leftrightarrow s(M) < 0, \ \ R_0 > 1 \Leftrightarrow s(M) > 0. \quad (11)$$

Clearly, it is evident that it suffices to prove the conditions (A1)–(A5) from Ref. [20]. Conditions (A1)–(A4) are obviously satisfied, therefore, it remains to demonstrate that matrix

$$J|_{P_0} = \begin{pmatrix} J_1 & J_2 \\ 0 & M \end{pmatrix}_{(4m\times 4m)} \quad (12)$$

has all eigenvalues with negative real parts, where

$$J_1 = \begin{pmatrix} -\delta_{1v} & P(2|1)d_{21} & \cdots & P(m|1)d_{m1} \\ 2P(1|2)d_{12} & -\delta_{2v} & \cdots & 2P(m|2)d_{m2} \\ \vdots & \vdots & \ddots & \vdots \\ mP(1|m)d_{1m} & mP(2|m)d_{2m} & \cdots & -\delta_{mv} \end{pmatrix}_{(m\times m)} - \mathrm{diag}(d_{kv})_{(m\times m)}, \quad (13)$$

$$J_2 = \begin{pmatrix} -F_1 & -F_2 & -F_3 \end{pmatrix}_{(m\times 3m)}. \quad (14)$$

According to Eq. (3), the matrix (13) is strictly diagonally dominant by columns, and $-d_{kv} - \delta_{kv} < 0$. Similarly to Theorem 2, all eigenvalues of J_1 are negative. When $R_0 < 1$, $s(M) < 0$, which implies $s(J|_{P_0}) < 0$. Therefore, the equilibrium P_0 of system (2) is locally asymptotically stable.

Next, we will prove that p_0 is globally attractive when $R_0 < 1$, that is, for any k, when $1 \le k \le m$, the following inequality holds:

$$\lim_{t\to\infty}(S_k(t), E_k(t), I_k(t), W_k(t)) = (S_k^0, 0, 0, 0). \quad (15)$$

From system (2), it can be deduced

$$\frac{\mathrm{d}S_k}{\mathrm{d}t} \le A_k - d_{kv}S_k - \delta_k S_k + k\sum_{k'=1}^{m} P(k'|k)d_{k'k}S_{k'}, \quad 1 \le k \le m. \quad (16)$$

Considering the following linear system:

$$\frac{\mathrm{d}S_k}{\mathrm{d}t} = A_k - d_{kv}S_k - \delta_k S_k + k\sum_{k'=1}^{m} P(k'|k)d_{k'k}S_{k'}, \quad 1 \le k \le m. \quad (17)$$

The Jacobian matrix of system (17) is

$$\begin{pmatrix} -d_{1v} - \delta_{1v} & P(2|1)d_{21} & \cdots & P(m|1)d_{m1} \\ 2P(1|2)d_{12} & -d_{2v} - \delta_{2v} & \cdots & 2P(m|2)d_{m2} \\ \vdots & \vdots & \ddots & \vdots \\ mP(1|m)d_{1m} & mP(2|m)d_{2m} & \cdots & -d_{mv} - \delta_{mv} \end{pmatrix}_{(m\times m)}. \quad (18)$$

Clearly, Jacobian matrix (18) is strictly diagonally dominant. Moreover, the main diagonal elements $-d_{kv} - \delta_{kv} < 0$ of matrix (18), implying that system (17) has a unique positive equilibrium $S^0 = (S_1^0, \cdots, S_m^0)^{\mathrm{T}}$. Since system (17) is linear, the disease-free equilibrium S^0 is globally asymptotically stable. For any $\eta > 0$, there exists a sufficiently large t such that $S_k(t) \le S_k^0 + \eta$, $1 \le k \le m$. Therefore, for sufficiently large t, the following auxiliary system holds:

$$\begin{cases} \frac{\mathrm{d}E_k}{\mathrm{d}t} \le \beta_k(E_k + I_k)(S_k^0(t) + \eta) + \alpha_k(S_k^0(t) + \eta)W_k \\ \qquad - \delta_k E_k - \theta_k E_k - d_{kv}E_k + k\sum\limits_{k'=1}^{m} P(k'|k)d_{k'k}E_{k'}, \\ \frac{\mathrm{d}I_k}{\mathrm{d}t} = \theta_k E_k - \mu_k I_k - d_{kv}I_k, \\ \frac{\mathrm{d}W_k}{\mathrm{d}t} = \gamma_k(E_k + I_k) - \omega W_k. \end{cases} \quad (19)$$

Next, we prove that the positive solutions of the auxiliary system (19) tend to zero as $t \to \infty$. We define

$$M_\eta = \begin{pmatrix} M_1 & M_2 & M_3 \\ 0 & 0 & 0 \\ 0 & 0 & 0 \end{pmatrix}_{(3m\times 3m)}, \quad (20)$$

$$M_1 = M_2 = \mathrm{diag}(\beta_k S_k^0 \eta)_{(m\times m)}, \quad (21)$$

$$M_3 = \mathrm{diag}(\alpha_k S_k^0 \eta)_{(m\times m)}. \quad (22)$$

According to Ref. [20], when $R_0 < 1$, $s(M) < 0$. For sufficiently small η, $s(M + M_\eta)$ is continuous. Taking a small $\eta > 0$ such that $s(M + M_\eta) < 0$. Based on the Perron–Frobenius theorem, all eigenvalues of the matrix $M + M_\eta$ have negative real parts when $s(M + M_\eta) < 0$. Therefore, for any k, when $1 \le k \le m$, system (19) satisfies the following inequality:

$$(E_k'(t), I_k'(t), W_k'(t)) \to (0, 0, 0), \ \ t \to \infty. \quad (23)$$

It implies that the zero solution of system (19) is globally asymptotically stable. For any k, when $1 \le k \le m$, using the comparison principle,[22] we obtain

$$(E_k(t), I_k(t), W_k(t)) \to (0,0,0), \quad t \to \infty. \tag{24}$$

For any k, when $1 \le k \le m$, by the theory of asymptotic autonomous systems,[23] we can conclude

$$(S_k(t), E_k(t), I_k(t), W_k(t)) \to (S_k^0, 0, 0, 0), \quad t \to \infty. \tag{25}$$

In other words, when $R_0 < 1$, the disease-free equilibrium P_0 is globally attractive. Furthermore, considering the local asymptotic stability of the disease-free equilibrium, we conclude that P_0 is globally asymptotically stable when $R_0 < 1$. This completes the proof.

3.3. The existence of endemic equilibrium

This section proves that system (2) has at least one positive equilibrium point when $R_0 > 1$. We define

$$\begin{aligned}
X = \{&(S_1, E_1, I_1, W_1, \ldots, S_m, E_m, I_m, W_m) : \\
&S_k > 0, E_k \ge 0, I_k \ge 0, W_k \ge 0, 1 \le k \le m\}, \\
X_0 = \{&(S_1, E_1, I_1, W_1, \ldots, S_m, E_m, I_m, W_m) : \\
&(S_1, E_1, I_1, W_1, \ldots, S_m, E_m, I_m, W_m) \in X, \\
&E_k > 0, I_k > 0, W_k > 0, 1 \le k \le m\}, \\
\partial X_0 = X \backslash X_0 = \{&(S_1, E_1, I_1, W_1, \ldots, S_m, E_m, I_m, W_m) : \\
&(S_1, E_1, I_1, W_1, \ldots, S_m, E_m, I_m, W_m) \in X, \\
&\text{for some } k \in \{1, \ldots, m\}, E_k = 0, \text{ or } I_k = 0, \text{ or } W_k = 0\}.
\end{aligned}$$

Theorem 4 When $R_0 > 1$, there exists a positive constant ε such that when $\|(E_k(0), I_k(0), W_k(0))\| < \varepsilon$ for all initial values $(S_k(0), E_k(0), I_k(0), W_k(0)) \in X_0$ and for $1 \le k \le m$, the following holds:

$$\limsup_{t \to \infty} \max_k \| (E_k(t), I_k(t), W_k(t)) \| > \varepsilon. \tag{26}$$

Proof Considering an auxiliary system

$$\begin{aligned}
\frac{\mathrm{d}S_k}{\mathrm{d}t} &= A_k - 2\beta_k S_k \varepsilon_1 - \alpha_k S_k \varepsilon_1 - d_{kv} S_k - \delta_k S_k \\
&\quad + k \sum_{k'=1}^{m} P(k'|k) d_{k'k} S_{k'}, \quad 1 \le k \le m,
\end{aligned} \tag{27}$$

where ε_1 is a positive number to be determined. Similarly to system (17), system (27) has a unique global asymptotically stable positive equilibrium point $S^0(\varepsilon_1) = (S_1^0(\varepsilon_1), \ldots, S_m^0(\varepsilon_1))^{\mathrm{T}}$. According to the implicit function theorem, $S^0(\varepsilon_1)$ is continuous. Therefore, further restricting ε_1 small enough ensures $S_k(\varepsilon_1) > S_k^0 - \eta$ for $1 \le k \le m$. For $t > T_1$, there exists $T_1 > 0$ such that $S_k(t) > S_k^0 - \eta$. Therefore, when $t > T_1 + T$, we have

$$\begin{cases}
\frac{\mathrm{d}E_k}{\mathrm{d}t} \ge \beta_k (E_k + I_k)(S_k^0 - \eta) + \alpha_k (S_k^0 - \eta) W_k - \delta_k E_k \\
\qquad\qquad - \theta_k E_k - d_{kv} E_k + k \sum\limits_{k'=1}^{m} P(k'|k) d_{k'k} E_{k'}, \\
\frac{\mathrm{d}I_k}{\mathrm{d}t} = \theta_k E_k - \mu_k I_k - d_{kv} I_k, \\
\frac{\mathrm{d}W_k}{\mathrm{d}t} = \gamma_k (E_k + I_k) - \omega W_k.
\end{cases} \tag{28}$$

Consider the following system:

$$\begin{cases}
\frac{\mathrm{d}E_k}{\mathrm{d}t} = \beta_k (E_k + I_k)(S_k^0 - \eta) + \alpha_k (S_k^0 - \eta) W_k - \delta_k E_k \\
\qquad\qquad - \theta_k E_k - d_{kv} E_k + k \sum\limits_{k'=1}^{m} P(k'|k) d_{k'k} E_{k'}, \\
\frac{\mathrm{d}I_k}{\mathrm{d}t} = \theta_k E_k - \mu_k I_k - d_{kv} I_k, \\
\frac{\mathrm{d}W_k}{\mathrm{d}t} = \gamma_k (E_k + I_k) - \omega W_k.
\end{cases} \tag{29}$$

According to $R_0 > 1 \Leftrightarrow s(M) > 0$, we can find a sufficiently small η such that $s(M - M_\eta) > 0$, where M_η is defined as shown in Eqs. (20)–(22). Because $s(M - M_\eta) > 0$, when $1 \le k \le m$:

$$(E_k'(t), I_k'(t), W_k'(t)) \to (\infty, \infty, \infty), \quad t \to \infty. \tag{30}$$

Using the comparison principle,[22] we obtain

$$(E_k(t), I_k(t), W_k(t)) \to (\infty, \infty, \infty), \quad t \to \infty. \tag{31}$$

This leads to a contradiction, which establishes the validity of Eq. (26). Thus, the proof is complete.

Theorem 5 When $R_0 > 1$, system (2) has at least one positive equilibrium, and there exists a constant ε such that every solution of system (15) with respect to X_0 satisfies

$$\min\left\{ \liminf_{t \to \infty} \inf_k E_k(t), \liminf_{t \to \infty} \inf_k I_k(t), \liminf_{t \to \infty} \inf_k W_k(t) \right\} \ge \varepsilon, \quad 1 \le k \le m.$$

Proof Firstly, we establish the uniform persistence of system (2) with respect to $(X_0, \partial X_0)$. Clearly, X and X_0 are positively invariant and ∂X_0 is relatively closed in X_0. By theorem 1, system (2) is point dissipative. Let $M_\partial = \{(S_1(t), E_1(t), I_1(t), W_1(t), \ldots, S_m(t), E_m(t), I_m(t), W_m(t)) : (S_1(t), E_1(t), I_1(t), W_1(t), \ldots, S_m(t), E_m(t), I_m(t), W_m(t)) \in \partial X_0, \forall t \ge 0\}$. Next, we proceed to prove the following equation:

$$\begin{aligned}
M_\partial = \{&(S_1(t), 0, 0, 0, \ldots, S_m(t), 0, 0, 0) : S_k(t) \ge 0, \\
&1 \le k \le m\}.
\end{aligned} \tag{32}$$

Clearly, $\{(S_1(t), 0, 0, 0, \ldots, S_m(t), 0, 0, 0) : S_k(t) \ge 0, 1 \le k \le m\} \subset M_\partial$, Next, we need to prove that $M_\partial \subset \{(S_1(t), 0, 0, 0, \ldots, S_m(t), 0, 0, 0) : S_k(t) \ge 0, 1 \le k \le m\}$. Assuming $(S_1(t), E_1(t), I_1(t), W_1(t), \ldots, S_m(t), E_m(t), I_m(t), W_m(t)) \in M_\partial$, thus, for $1 \le k \le m$, we have $E_k(t) = I_k(t) = W_k(t) = 0, \forall t \ge 0$. If this assumption does not hold, then there exists a k and a t_0 such that either $E_k(t_0)$, $I_k(t_0)$, or $W_k(t_0)$ is greater

than 0. We divide $(1,\ldots,m)$ into sets Q_1 and Q_2, where Q_1 and Q_2 satisfy the following conditions:

$$(E_k(t_0),I_k(t_0),W_k(t_0))^{\mathsf{T}}=(0,0,0)^{\mathsf{T}},\ \ \forall k\in Q_1, \tag{33}$$

$$E_k(t_0)>0,\ \text{or}\ I_k(t_0)>0,\ \text{or}\ W_k(t_0)>0,\ \ \forall k\in Q_2. \tag{34}$$

From the definition of M_∂, it is evident that Q_1 is not empty. The earlier assumption stated that there exist a k and a t_0 such that $E_k(t_0)$, $I_k(t_0)$, or $W_k(t_0)$ is greater than 0, hence Q_2 is not empty.

For $k\in Q_2$, we assume $E_k(t_0)>0$, $I_k(t_0)=W_k(t_0)=0$. According to the system (2), we have $I_k'(t_0)=\theta_k E_k(t_0)>0$, $W_k'=\gamma_k E_k(t_0)>0$. Therefore, there exists a relatively small positive number ε_0 such that $E_k(t)>0, I_k(t)>0, W_k(t)>0$, $k\in Q_2$ for $t_0<t<t_0+\varepsilon_0$.

For $k\in Q_1$, $E_k'(t_0)\geq P(k'|k)d_{k'k}E_k(t_0)>0$. Therefore, there exists a positive number ε_1 such that $E_k(t)>0$ for $t_0<t<t_0+\varepsilon_1$. Similarly, there exists ε_1 such that $I_k(t)>0$, $W_k(t)>0$. This implies that if we take $\varepsilon_m=\min\{\varepsilon_0,\varepsilon_1,\varepsilon_2\}$, then $(S_1(t),E_1(t),I_1(t),W_1(t),\ldots,S_m(t),E_m(t),I_m(t),W_m(t))\notin\partial X_0$ for $t_0<t<t_0+\varepsilon_m$. This contradicts the assumption; hence, equation (32) holds true.

Combining the global asymptotic stability of the disease-free equilibrium point P_0 of system (2), the set M_∂ contains only one equilibrium point P_0, which is an isolated invariant set in X, meaning $W^S(P_0)\cap X_0=\varnothing$. Every trajectory in M_∂ converges to P_0, and P_0 is non-cyclic in M_∂. According to Theorem 4.6 in Ref. [24], system (2) is uniformly persistent with respect to $(X_0,\partial X_0)$.

According to Theorem in 2.4 in Ref. [25], system (2) has an equilibrium $(S^*,E^*,I^*,W^*)\in X_0$, where $S^*=(S_1^*,\ldots,S_m^*)$, $E^*=(E_1^*,\ldots,E_m^*)$, $I^*=(I_1^*,\ldots,I_m^*)$, $W^*=(W_1^*,\ldots,W_m^*)$. Assuming $S_k^*=0$ for $1\leq k\leq m$, from the first equation of system (2), we obtain $0=-\delta_k E_k-\theta_k E_k-d_{kv}E_k+k\sum_{k'=1}^{m}P(k'|k)d_{k'k}E_{k'}$. This leads to $I_k^*=0$, a contradiction. Therefore, by the irreducibility of the coefficient matrix and the first equation of system (2), we conclude $S_k^*>0$ for $1\leq k\leq m$. Hence, (S^*,E^*,I^*,W^*) is a positive equilibrium of system (2). This completes the proof.

4. Numerical simulation

We choose Heilongjiang province as an example to investigate the transmission of brucellosis based on sheep movement among 12 administrative regions including Harbin, Qiqihar, Shuangyashan, Daqing, Jiamusi, Qitaihe, Mudanjiang, Heihe, Suihua, Daxing'anling, Jixi, and Yichun, as Heilongjiang province is a high-risk area for brucellosis.[3] First, the parameters are given by fitting the actual data to the model based on the BA network, the ER network, and homogeneous mixing network. Then, we simulate the impact of the network average degree on the transmission of brucellosis and the impact of parameters on R_0.

4.1. Parameter estimation and fitting results

In this section, system (1) is applied to fit the cumulative cases of human brucellosis in Heilongjiang province from 2010 to 2020. The data comes from the Chinese Center for Disease Control and Prevention Information System, with the link https://www.chinacdc.cn/. The unknown parameters in the model are estimated using the least squares method, and all parameter values are expressed as units of year, as shown in Table 1. According to the results of the 6th population census, population data for the 12 regions of Heilongjiang in 2010 are obtained. Based on data from the brucellosis outbreak in these regions in 2010, initial data from the susceptible human population and infected human data are obtained. Since there is no data available for infected sheep, estimates are made of the numbers of exposed and infected sheep during the incubation period. Regarding the quantity of brucella in the environment, it is assumed to range from 1×10^6 to 1.2×10^6. Twelve values are randomly selected within this range to represent the initial quantity of brucella in the environment. The data mentioned earlier all come from the Heilongjiang Provincial Bureau of Statistics, with the link https://tjj.hlj.gov.cn/tjjnianjian/2020/zk/indexch.htm.

Table 1. Parameter variable values and descriptions.

Parameter	Description	Value	Source
θ_k	the rate of clinical outcome of exposed sheep within a subpopulation of degree k	1	[26]
μ_k	disease-related culling rate of infectious sheep within a subpopulation of degree k	0.25	[27]
γ_k	the amount of brucella per unit time emitted by exposed and infected sheep within a subpopulation of degree k	15	[26]
ω	brucella decay rate	3.6	[26]
p	the recovery rate of the infected population	0.6	[28]
d	the natural mortality rate of humans	0.0065	[29]
d_{kv}	the sale rate of sheep within a subpopulation of degree k	0.4508	[30]
α_k	brucella in environment-to-susceptible sheep transmission rate within a subpopulation of degree k	1.7×10^{-10}	[26]
α_{hk}	brucella in environment-to-susceptible human transmission rate within a subpopulation of degree k	1×10^{-11}	[26]

For the 12 cities in Heilongjiang province, we construct a BA network with an average degree of 5 and an ER network

with an average degree of 4.833, and the network schematic diagram is shown in Fig. 4. The sheep are transported in these two heterogeneous networks. In order to compare with traditional dynamics, we also consider the case of homogeneous mixing network.[32] According to the parameter values shown in Table 1, the model solutions are adapted to the cumulative human brucellosis cases reported from 2010 to 2020 in the 12 Heilongjiang regions using Matlab in these three networks. The parameter values are obtained as follows. β_k are 5.267×10^{-7}, 5.746×10^{-7} and 6.091×10^{-7}, respectively, β_{hk} are 1.437×10^{-7}, 1.322×10^{-7} and 1.31×10^{-7}, respectively; δ_k are 0.15, 0.1712 and 0.1926, respectively.

Figure 5 presents the numerical fit and 95% confidence interval for the cumulative cases of human brucellosis reported in the 12 regions of Heilongjiang from 2010 to 2020. As shown, the model solution aligns well with the actual data, demonstrating that the model is relatively reasonable. Furthermore, based on parameter estimates, the basic reproduction numbers under sheep transport scenarios for BA network, ER network, and homogeneous mixing network are 1.7594, 1.8477, and 1.8586, respectively, all of which exceed 1. This consistently suggests that as long as sheep transport occurs, brucellosis will continue to spread between regions. Furthermore, the comparison shows that the basic reproduction number is highest in the homogeneous mixing network, which facilitates the spread of brucellosis, whereas it is lowest in the BA network, which can mitigate the spread of brucellosis between regions.

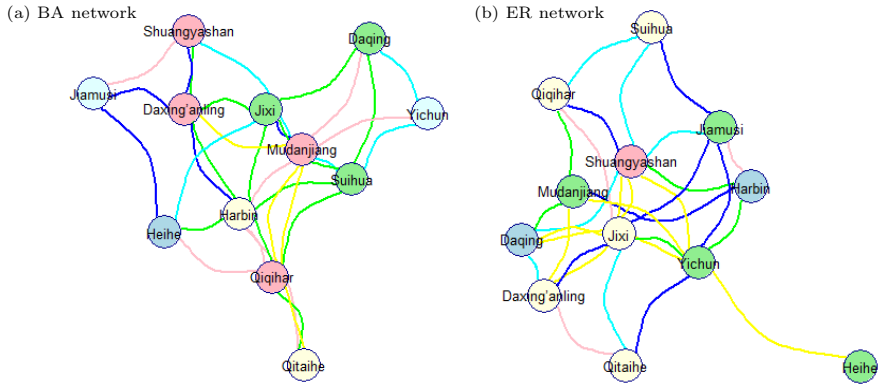


Fig. 4. The network diagram of the 12 cities in Heilongjiang province.

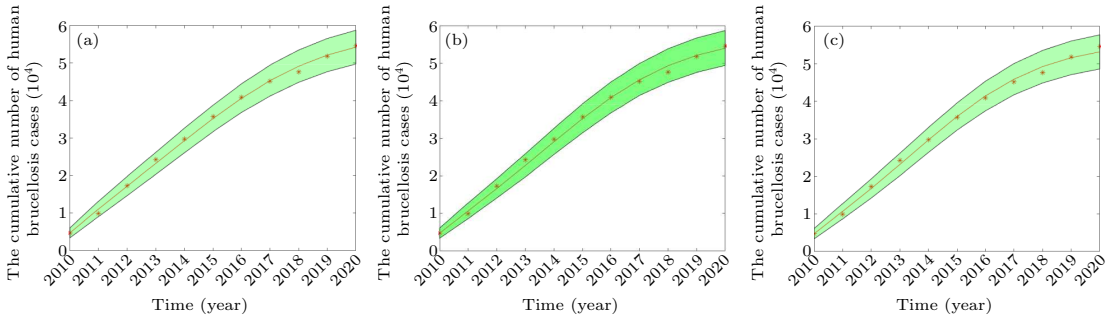


Fig. 5. The fitting results of the cumulative human brucellosis cases in Heilongjiang province from 2010 to 2020 are shown. The red line represents the model's solution, the dots indicate the actual data points, and the shaded area denotes the 95% confidence interval.

4.2. The impact of network average degree on the transmission of brucellosis

In this section, we conduct simulations on 1000 Barabsi–Albert (BA) and 1000 Erds–Rnyi (ER) networks to observe how changes in the average degree of the network affect the disease transmission threshold and the number of infectious disease cases, as illustrated in Fig. 6. The data is smoothed using cubic spline interpolation, and the specific parameter values are provided in Tables 1 and 2. As shown in Fig. 6(a), when sheep herds are transported within BA networks, the basic reproduction number and cumulative cases initially decrease, followed by two fluctuations as the average degree remains below 5. Once the average degree exceeds 5, both the basic reproduction number and cumulative cases stabilize. Figure 6(b) demonstrates that in ER networks, the basic reproduction number and cumulative cases experience significant fluctuations when the average degree is below 2, with a peak occurring at an average degree of 2. As the average degree increases beyond 4, both values tend to stabilize. In summary, in both BA and ER networks, the basic reproduction number and cumulative cases tend to stabilize when the average degree is around 4 or 5. Furthermore, when the average degree reaches 11 in both BA and ER networks — equivalent to a homogeneous mixing network — the basic reproduction numbers are 1.7259, 1.8162, and 1.8586, and the cumulative case numbers are 54385, 54264, and 53135, respectively.

Table 2. The results of parameter estimation.

Parameter	Description	BA network	ER network	Uniform mixing network	Source
β_k	the infectious sheep-to-susceptible sheep transmission rate within a subpopulation of degree k	5.267×10^{-7}	5.746×10^{-7}	6.091×10^{-7}	fitted
β_{hk}	the infectious sheep-to-susceptible human transmission rate within a subpopulation of degree k	1.437×10^{-7}	1.322×10^{-7}	1.31×10^{-7}	fitted
δ_k	the sheep mobility rate within a subpopulation of degree k per unit time	0.15	0.1712	0.1926	fitted

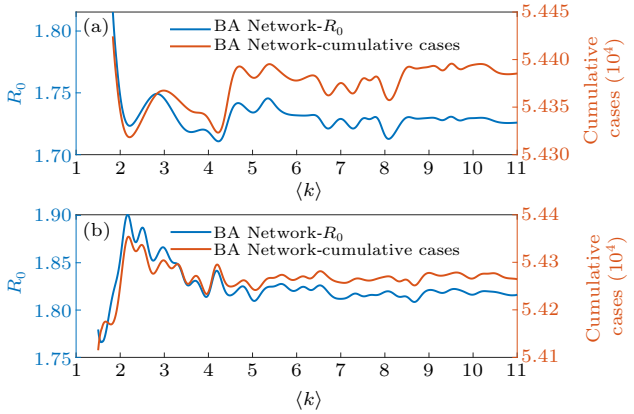


Fig. 6. The effect of the network's average degree on the spread of brucellosis is illustrated. The red and blue solid lines represent the influence of the average degree on the cumulative number of human brucellosis cases and the basic reproduction number, respectively.

4.3. The impact of parameters on R_0

Next, sensitivity analysis of the basic reproduction number is conducted to study the factors influencing the inter-regional spread of brucellosis. In this section, we use the partial rank correlation coefficient (PRCC) to analyze the sensitivity of the basic reproduction number R_0 to the control parameters. The control parameters are the sheep mobility rate within the subpopulation of degree k per unit time δ_k, the sale rate of sheep d_{kv}, disease-related culling rate of infectious sheep μ_k, the infectious sheep-to-susceptible sheep transmission rate β_k, the infectious sheep-to-susceptible human transmission rate β_{hk}. The higher the PRCC value, the greater the impact of the parameter on R_0. The results of the analysis are shown in Fig. 7. R_0 is more sensitive to the mobility rate δ, the sale rate d_{kv}, the culling rate μ, and the infection rate β. The absolute values of PRCC are all greater than 0.5, and R_0 is negatively correlated with the mobility rate δ, the sale rate d_{kv}, culling rate μ, but positively correlated with the infection rate β. Therefore, we will focus on studying the impact of changes in the four parameters with large absolute PRCC values on R_0 in these three types of transport networks.

Based on the conclusions drawn from Fig. 7, we analyze how the basic reproduction number (R_0) is affected by the mobility rate δ, the sale rate d_{kv}, the culling rate μ and the infection rate β when sheep are transported in networks generated by different models, that is, the BA network, the ER network, and the homogeneous mixing network. As shown in Fig. 8(a), when the sales rate d_{kv} is less than 0.2, R_0 increases significantly with increasing sales rates, then declines before again increasing. Above a sale rate of 0.2, R_0 decreases as the sale rate increases. Regardless of the sale rate d_{kv}, R_0 is lowest in BA networks and highest in homogeneous mixing networks. In Fig. 8(b), the infection rate β also positively affects R_0, with the highest R_0 in BA networks and the lowest in homogeneous mixing networks at equivalent infection rates β. In contrast, in Figs. 8(c) and 8(d), R_0 decreases with a higher culling rate μ and mobility rates δ, with BA networks minimizing and homogeneous mixing networks maximizing R_0. This indicates that the transport of sheep under a homogeneous mixing network will accelerate the spread of brucellosis over the region and the transport of sheep under the BA network can effectively control the spread of brucellosis over the region. In addition, under these three network mechanisms, R_0 decreases with the increase of the mobility rate δ, which is opposite to the conclusion drawn by Zhang, Guo, Qin *et al.*[4,10,11] that the basic reproduction number increases with the increase of the mobility rate δ when there is transport of sheep between the patch. To explore the reasons for this research result, we analyzed the values and changes in basic reproduction numbers of each subpopulation (cities in Heilongjiang province) under this transportation mechanism.

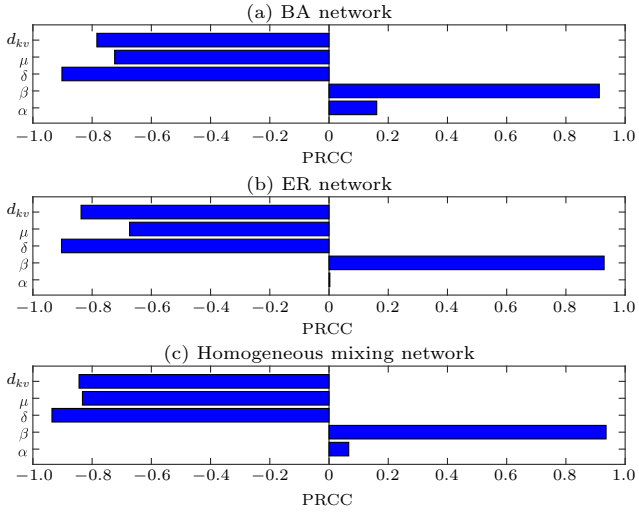


Fig. 7. Sensitivity analysis of the basic reproduction number R_0 using partial rank correlation coefficient (PRCC).

Then, we primarily study the impact of transportation rate on the basic reproduction number of 12 cities in Heilongjiang under three network structures: BA network, ER network, and

homogeneous mixing network. The results of the analysis are shown in Fig. 9. In these three network structures, the basic reproduction number of cities such as Qiqihar, Daqing, Jiamusi, Heihe, and Suihua shows a consistent trend with the basic reproduction number of the entire Heilongjiang province, decreasing as the mobility rate increases. Combining actual data, we found that these cities have significantly higher breeding volume and initial cases compared to other cities. As a result, when the mobility rate increases, the number of infected and exposed sheep transferred is higher, and the transmission of disease in this city is controlled. These cities with a higher breeding volume are also the main drivers of the overall epidemic trend in Heilongjiang province. Similarly, cities such as Shuangyashan, Qitaihe, Daxinganling, Jixi, and Yichun have a relatively low breeding volume. When the mobility rate increases, the number of infected and exposed sheep transferred out is much smaller than those transferred in, increasing the spread of the disease within the city. That is, the basic reproduction number increases with the mobility rate. In Mudanjiang, where the breeding volume is close to the average level, the basic reproduction number first increases and then decreases with the mobility rate. This indicates that when transportation reaches a certain level, reducing transportation can prevent the spread of brucellosis in the city.

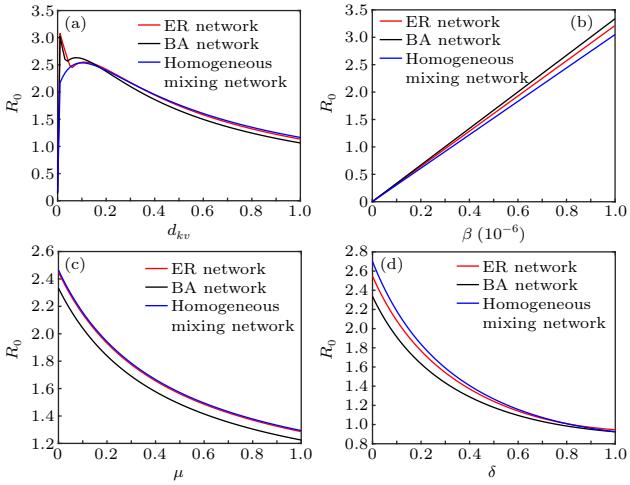


Fig. 8. Sensitivity analysis of the basic reproduction number R_0. The effects of (a) the sale rate d_{kv}, (b) infection rate β, (c) culling rate μ, and (d) the mobility rate δ on the basic reproduction number R_0.

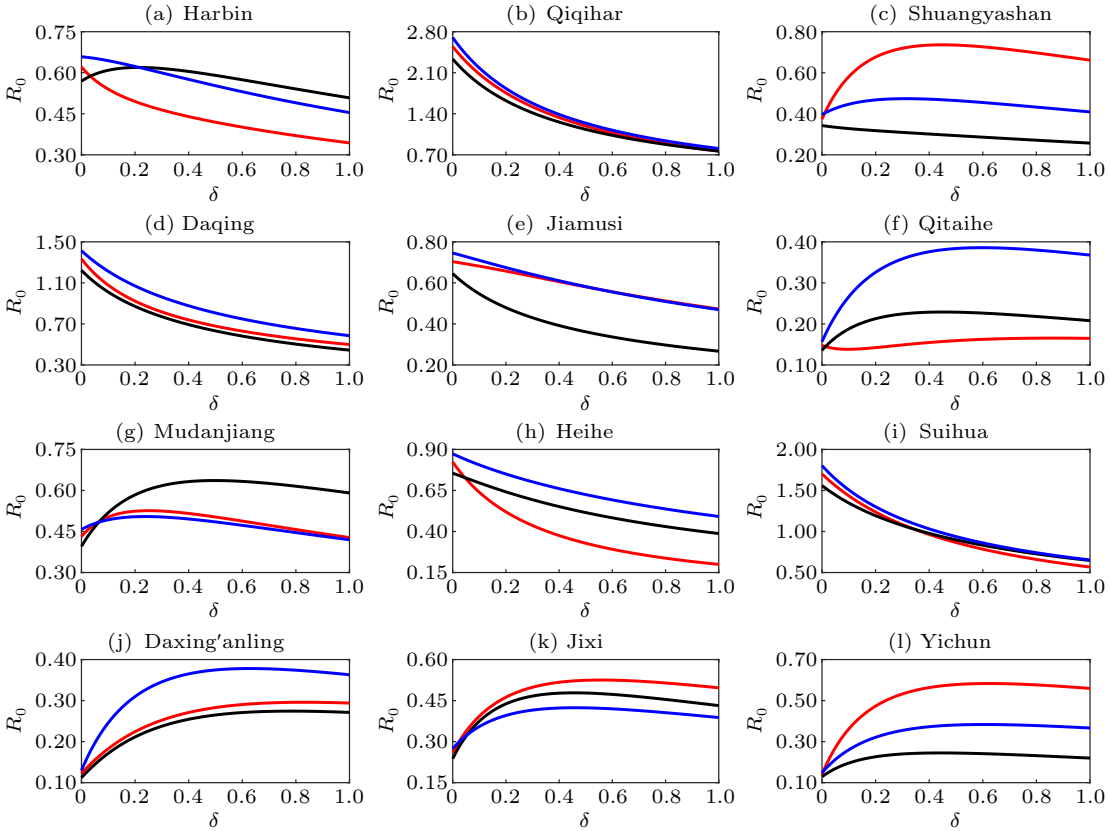


Fig. 9. The impact of sheep transportation on the spread of brucellosis. The red solid line, black solid line, and blue solid line represent the impact of the transportation rate on the basic reproduction number for each city during the transportation of sheep in ER network, BA network, and homogeneous mixing network, respectively.

In summary, in areas with high incidence of the disease, it is possible to adjust the sheep transportation network to control the spread of the disease. For areas where the disease spreads rapidly, the culling rate can be appropriately increased to control the spread of the disease. Additionally, the transportation of sheep between subpopulations is not always harmful to the control of brucellosis. For cities with a large breeding volume, moving sheep outward can actually control the spread of bru-

cellosis locally. In addition, the epidemic trend in cities with a larger breeding volume significantly impacts the overall epidemic trend in the province and should be given priority for monitoring. At the same time, cities with a smaller breeding volume should be encouraged to expand their breeding scale, thus reducing the development of their own epidemics during frequent animal trading.

5. Conclusion

The increase in livestock breeding and the frequent cross-regional transport of animals have facilitated the spread of brucella between regions, leading to an increase in cases of brucellosis and an expanded spatial transmission range.[4,5] To analyze the impact of sheep transportation on the spread of brucellosis, we construct a human–sheep coupled brucellosis model in metapopulation networks. Theoretically, we explore the positive invariant set, the basic reproduction number, and the existence, uniqueness, and stability of disease-free equilibrium, and the existence of the endemic equilibrium of the system.

In practical terms, the Heilongjiang province is used as a case study for numerical simulations. Based on data fitting and parameter estimation using the least squares method, the basic reproduction number was calculated to be 1.7594, 1.8477, and 1.8586 for sheep transportation in the BA network, the ER network, and the homogeneous mixing network, respectively. The results show that when sheep are transported in the homogeneous mixing network, the basic reproduction number is the highest, accelerating the spread of brucellosis across regions. In contrast, transportation in the BA network slows the spread between regions.

A parameter sensitivity analysis led to the following conclusions. First, increasing the sales rate d_{kv} and the culling rate μ can help control the spread of brucellosis to some extent. Second, the average degree of the network affects the transmission dynamics, with transportation in a BA network with an average degree greater than 5 being particularly advantageous. Lastly, while sheep transportation can both promote and mitigate the spread of brucellosis, regional factors must be considered. In areas with a smaller livestock population, such as Shuangyashan and Qitaihe, reducing sheep outflow and moderately expanding breeding operations are recommended. In contrast, in regions with larger populations, such as Qiqihar, Daqing and Suihua, increasing sheep outflow with proper monitoring can help control the spread of brucellosis.

In summary, the model and simulation results presented in this article offer valuable insight to livestock farmers, providing strategies rooted in the dynamics of network transmission to mitigate the spread of brucellosis during animal trade. These findings have practical significance for controlling the disease in livestock populations.

Program availability

The source code is openly available in Science Data Bank at https://doi.org/10.57760/sciencedb.16944.

Acknowledgments

Project supported by the National Natural Science Foundation of China (Grant No. 12101443,12371493) and the Natural Science Foundation of Shanxi Province (Grant Nos. 20210302124260 and 202303021221024).

References

[1] Robertson A 1976 *Handbook on Animal Diseases in the Tropics*, 3rd Edn. (London: Veterinary) p. 96
[2] Pappas G and Papadimitriou P 2007 *Int. J. Antimicrob. Agents* **30** 29
[3] Sun G Q, Li M T, Zhang J, Zhang W, Pei X and Jin Z 2020 *Comput. Struct. Biotechnol. J.* **18** 3843
[4] Zhang J, Ruan S G, Sun G Q, Sun X D and Jin Z 2014 *Journal of Shanghai Normal University* **43** 441
[5] Zeng H, Wang Y M, Sun X D, Liu P, Xu Q G, Huang D, Gao L, You S B and Huang B X 2019 *PLOS Neglected Tropical Diseases* **13** e0007285
[6] Ge J X, Ying S H, Tang L, Yuan S and Xing Z F 2023 *Chin. J. Public Health Eng.* **22** 6
[7] Suo B, Liu M, Wu C Y, Zhou K, Liu C M and Z X 2022 *J. Med. Pest Control* **38** 2
[8] Yin S H, Tang L, Yu Y L, Xing Z F Yuan S and Ge J X 2021 *Disease Surveil.* **36** 12
[9] Yang C L, Lolika P O, Mushayabasa S and Wang J 2017 *Nonlinear Anal. Real World Appl.* **38** 49
[10] Guo J M, Luo X F, Zhang J and Li M T 2022 *Mathematics* **10** 3436
[11] Qin Y Y, Pei X, Li M T and Chai Y Z 2022 *Math. Biosci. Eng.* **19** 6396
[12] Li M, Song Y R, Song B, Li R Q, Jiang G P and Zhang H 2024 *Chin. Phys. B* **33** 088902
[13] Yang P, Fan R G, Wang Y B and Zhang Y Q 2024 *Chin. Phys. B* **33** 070206
[14] Zhang Y Q, Wang X W, Wang Y N and Zheng W 2024 *Chin. Phys. B* **33** 070702
[15] Colizza V, Pastor-Satorras R and Vespignani A 2007 *Nat. Phys.* **3** 276
[16] Richard L 1969 *Bulletin of the Entomological Society of America* **15** 237
[17] Levins R 1970 *Extinction. In: Gesternhaber M (ed) Some mathematical problems in biology* (Providence, Rhode Island: American Mathematical Society) pp. 77–107
[18] Gallos L K and Argyrakis P 2004 *Phys. Rev. Lett.* **92** 138301
[19] Lentz H H K, Selhorst T and Sokolov I M 2012 *Phys. Rev. E* **85** 066111
[20] Dreessche P and Watmough J 2002 *Math. Bio* **180** 29
[21] Diekmann O, Heesterbeek J A and Roberts M G 2010 *J. Royal Soc. Interf.* **7** 873
[22] Waltman P E and Smith H L 1995 *The Theory of the Chemostat: Dynamics of Microbial Competition* (London: Cambridge University Press) pp. 99–102
[23] Thieme H R 1992 *J. Math. Biol.* **30** 755
[24] Thieme H R 2006 *Siam J. Math. Anal.* **24** 407
[25] Zhao X Q 1995 *Canad. Appl. Math. Quart.* **3** 473
[26] Hou Q, Sun X D, Zhang J, Liu Y J, Wang Y M and Jin Z 2013 *Math. Biosci.* **242** 51
[27] Zhou L, Fan M, Hou Q, Jin Z and Sun X D 2018 *Math. Biosci. Eng.* **38** 435
[28] Shi Y J, Lai S J, Chen Q L, Mu D, Li Y, Li X X, Yin W W and Yu H J 2017 *Chinese Center for Disease Control and Prevention* **242** 51
[29] The Heilongjiang Provincial Bureau of Statistics
[30] Wang L S, Li M T, Pei X, Zhang J, Sun G Q and Jin Z 2023 *Commun. Nonl. Sci. Numer. Simul.* **124** 107310
[31] Li M T, Sun G Q, Zhang J, Jin Z, Sun X D, Wang Y M, Huang B X and Zheng Y H 2014 *Math. Biosci. Eng.* **11** 1115
[32] Wang X F, Li X and Chen G R *2012 Network Science: An Introduction* 1st ed (Beijing: Higher Education Press) pp. 193–226, 272–276